AD-A078 634 AERONAUTICAL RESEARCH LABS MELBOURNE (AUSTRALIA) F/G 20/11
A SPECIAL CRACK TIP ELEMENT FOR THREE-DIMENSIONAL CRACK PROBLEM--ETC(U)
NOV 78 R JONES , R J CALLINAN
UNCLASSIFIED ARL/STRUC NOTE-374 NL

| OF |
AD
A078634

END
DATE
FILMED
1-80
DDC

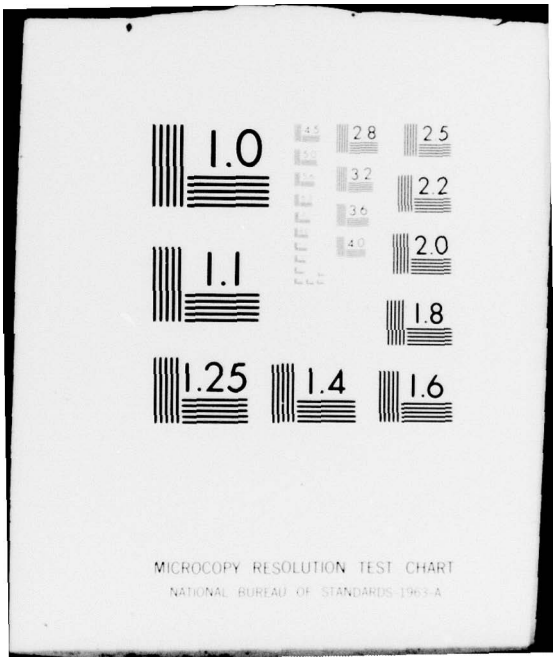
1.0
1.1
1.25
1.4
1.6
1.8
2.0
2.2
2.5
2.8
3.2
3.6
4.0
MICROCOPY RESOLUTION TEST CHART
NATIONAL BUREAU OF STANDARDS-1963-A

ARL-STRUC-NOTE-374 AR-001-319

(12)

DEPARTMENT OF DEFENCE

DEFENCE SCIENCE AND TECHNOLOGY ORGANISATION

AERONAUTICAL RESEARCH LABORATORIES

MELBOURNE, VICTORIA

STRUCTURES REPORT 374

A SPECIAL CRACK TIP ELEMENT FOR THREE-DIMENSIONAL CRACK PROBLEMS

by

R. JONES and R. J. CALLINAN

Approved for Public Release.

COPY No 1

NOVEMBER 1978

AR-001-319

DEPARTMENT OF DEFENCE
DEFENCE SCIENCE AND TECHNOLOGY ORGANISATION
AERONAUTICAL RESEARCH LABORATORIES

9 STRUCTURES REPORT 374

6 A SPECIAL CRACK TIP ELEMENT FOR THREE-DIMENSIONAL CRACK PROBLEMS.

11 Nov 78 12 26

by

10 Rhys Richard R. JONES and R. J. CALLINAN

14 ARL/STRUC NOTE-374

SUMMARY

This paper develops a finite element method for determining the stress intensity factors along the edge of a crack in an arbitrary three-dimensional body. A special element is placed around the crack front and in each special element the stresses and displacements are derived using the asymptotic nature of the stress and displacement fields near a crack tip.

The method is based on the authors' previous technique for evaluating the stress intensity factors in cracked sheets, and coincides with this method in the case of a through crack in a thin sheet. As illustrative examples the problems of a semicircular surface flaw and an internal penny shaped crack are considered. In each case the computed values of the stress intensity factors are in excellent agreement with known analytical results.

POSTAL ADDRESS: Chief Superintendent, Aeronautical Research Laboratories,
Box 4331, P.O., Melbourne, Victoria, 3001, Australia.

CONTENTS

NOTATION

E	Young's modulus.
ν	Poisson's ratio
K_1, K_2, K_3	Stress intensity factors
x, y, z	Cartesian co-ordinate system
r, θ, ϕ	Curvilinear co-ordinate system used to describe the crack
n, t, y	Curvilinear co-ordinate system treating the crack as the plane $y = 0$
σ_y, σ_n, σ_t, τ_{nt}, τ_{ny}, τ_{ty}	Stress components in the n, t, y co-ordinate system.
σ_{1n}, σ_{2n}, σ_{1y}, σ_{2y}, σ_{1t}, σ_{2t}, τ_{3ty}, τ_{3nt}, τ_{1ny}, τ_{2ny}	Coefficients of K_1, K_2, and K_3 in the expressions for the stresse along the crack front
u_n, u_t, u_y	Displacements in the n, t, and y directions
u_{1n}, u_{2n}, u_{1y}, u_{2y}, u_{3t}	Coefficients of K_1, K_2, and K_3 in the expressions for the u_n, u_t, and u_y displacements
J	Jacobian of the transformation from x, y, z co-ordinates to r, θ, and ϕ.
ϕ_e, ϕ_{e+1}	Upper and lower values of ϕ in the eth crack tip element
K_{1e}, K_{2e}, K_{3e}	Values of K_1, K_2, and K_3 at $\phi = \phi_e$
ψ_1, ψ_2	Linear interpolation functions of ϕ
u_0, v_0, w_0, ω_{xy}, ω_{xz}, ω_{yz}	Rigid body translations and rotations
u, v, w	Displacements in the x, y, z co-ordinate system
$\boldsymbol{\lambda}$	Vector containing the degrees of freedom of the crack tip element
V	Strain energy
K^e	Primitive stiffness matrix
L	Transformation matrix
σ	Applied stress
a	Half crack length
S	Strain energy density function
α	Direction of crack growth
rr, rl, y_0	Distances of the sides of the special element from the crack front

1. INTRODUCTION

Aircraft in service develop cracks from a variety of causes, such as fatigue or stress corrosion. In any given case there is a requirement to determine whether a crack is affecting the safe operation of the aircraft. The main theoretical tool for addressing such problems is fracture mechanics. Fracture mechanics is especially concerned with stresses in the immediate vicinity of a crack, which, in an elastic isotropic material, are known to have a singularity proportional to the square root of the distance from the crack front. These factors of proportionality, usually written as K_1, K_2, and K_3 and termed the stress intensity factors, occupy an important position in fracture mechanics and a great deal of effort has been spent on developing methods for obtaining them. Some of these methods are reviewed in References 1 and 2.

The present paper uses the finite element method, with a special element surrounding the crack front, to obtain the stress intensity factors K_1, K_2, and K_3. The analysis is an extension of the previous work described in References 3 and 4 and allows the special element to be of any arbitrary shape.

2. STRESS AND DISPLACEMENT FIELDS IN THE CRACKED ELEMENT

Let us consider an elliptical flaw, see Figure 1, and define a system of $x\ y\ z$ co-ordinates such that the xoz plane lies in the plane of the crack and the y axis is directed perpendicular to this plane.

If the semimajor and semiminor axes of the ellipse are of lengths a and b respectively then the equation of the crack front is given by

$$\frac{x^2}{a^2} + \frac{z^2}{b^2} = 1 \tag{1}$$

Let us also define a system of curvilinear co-ordinates r, θ and ϕ such that

$$y = r \sin \theta \tag{2}$$

$$x = a \cos \phi + r \cos \theta \cos \theta' \tag{3}$$

$$z = b \sin \phi + r \cos \theta \sin \theta' \tag{4}$$

where

$$\cos \theta' = b \cos \phi / \pi_0^{\frac{1}{2}} \tag{5}$$

$$\sin \theta' = a \sin \phi / \pi_0^{\frac{1}{2}} \tag{6}$$

and

$$\pi_0 = b^2 \cos \phi + a^2 \sin^2 \phi \tag{7}$$

In the r, θ, and ϕ co-ordinate system all points on the crack front have $r = 0$ and the parametric equation of the crack is

$$x = a \cos \phi \tag{8}$$

$$z = b \sin \phi \tag{9}$$

Consider two points P(r, θ, ϕ) and Q(r, θ, ϕ) with point P lying on the crack front. Then r is the distance from P to Q and θ is the angle between the line PQ and the normal $\mathbf{n}$ to the crack at P, see Figure 1.

Let us now consider a special crack tip element which is bounded above by the plane $\phi = \phi_e$ (= constant) and below by the plane $\phi = \phi_{e+1}$ (= constant). The element is polygonal

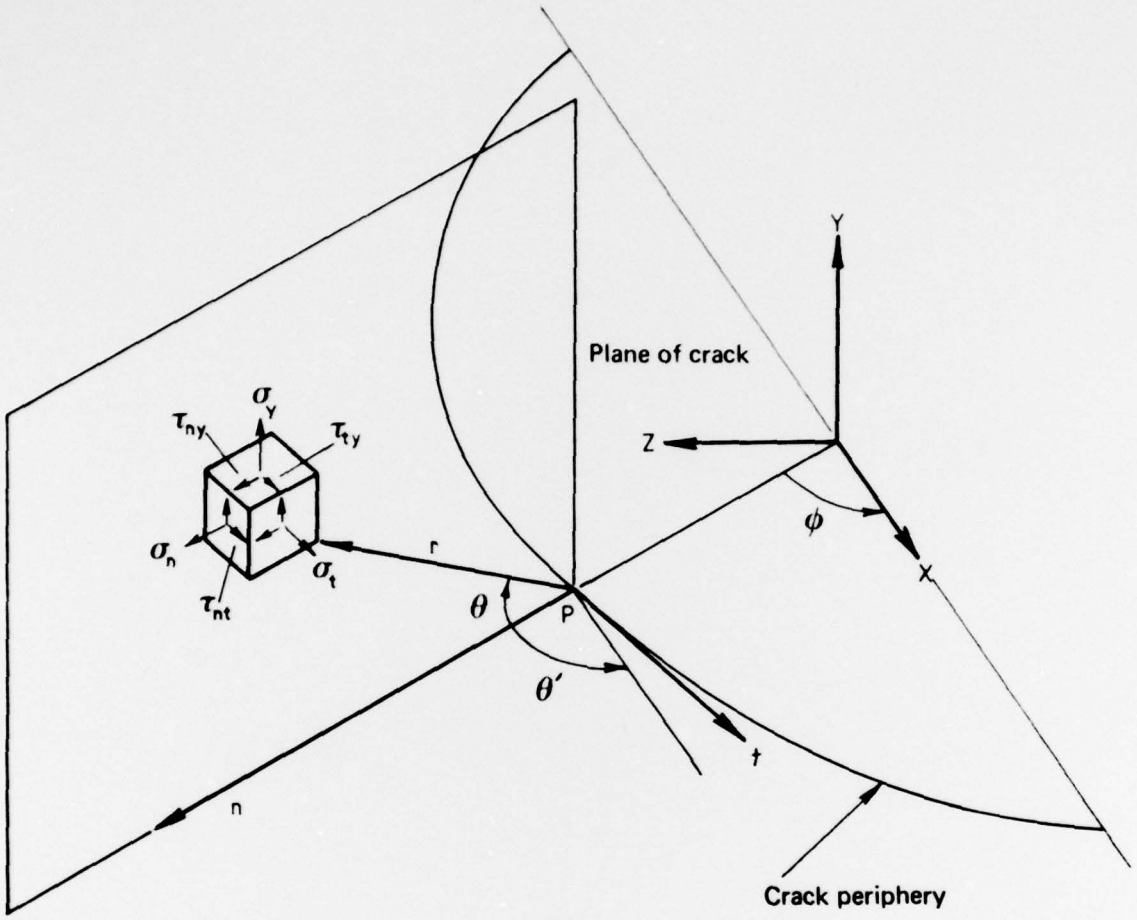

FIG. 1. STRESS COMPONENTS NEAR PERIPHERY OF CRACK, n AND t ARE NORMAL AND TANGENTIAL RESPECTIVELY TO THE PERIPHERY OF THE CRACK AT P AND LIE IN THE CRACK PLANE.

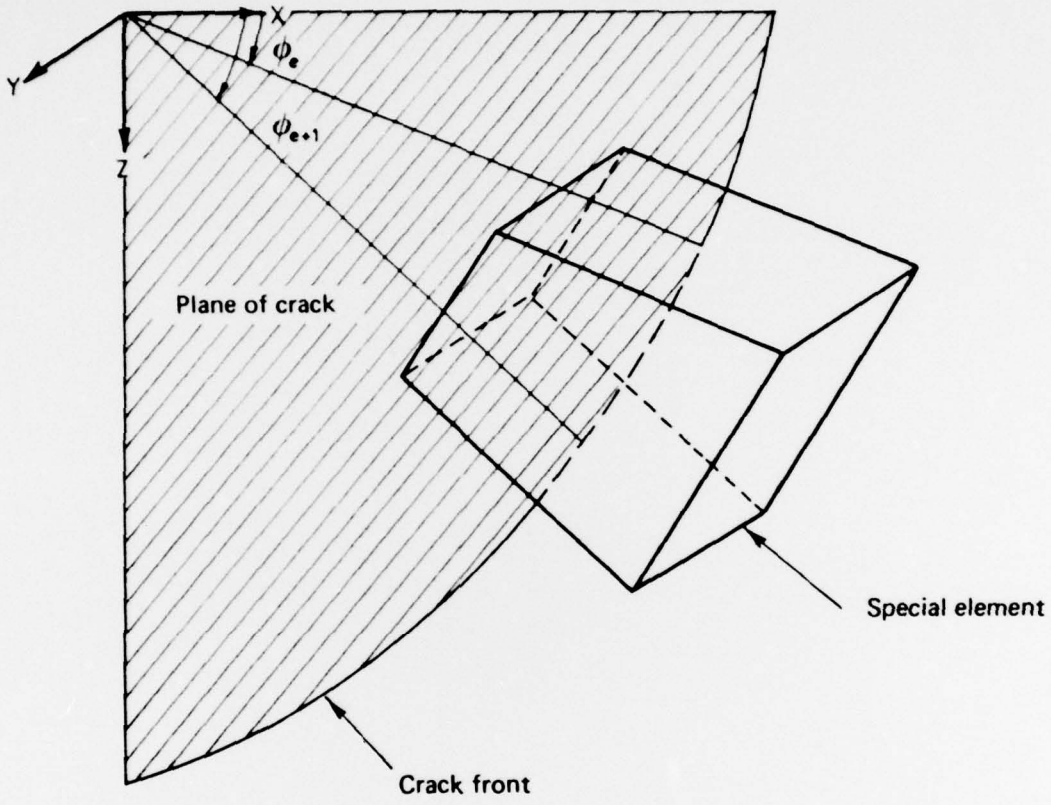

FIG. 2. GEOMETRY OF THE SPECIAL ELEMENT

in plan view and surrounds the crack front, see Figure 2. The special element shown in Figure 2 is also bounded by two planes both of which have y = const. and by two planes, which at the planes $\phi = \phi_e$ and $\phi = \phi_{e+1}$ have the same minimum distance from the crack front and which are perpendicular to the planes y = constant. A more detailed description of this element is given in the Appendix.

Within this element we will consider the stress and displacement fields to be given by the first term in their asymptotic expansions, see Reference 1, viz.

$$\sigma_n = K_1\sigma_{1n} + K_2\sigma_{2n} \tag{10}$$

$$\sigma_t = K_1\sigma_{1t} + K_2\sigma_{2t} \tag{11}$$

$$\sigma_y = K_1\sigma_{1y} + K_2\sigma_{2y} \tag{12}$$

$$\tau_{ny} = K_1\tau_{1ny} + \tau_{2ny} \tag{13}$$

$$\tau_{nt} = K_3\tau_{3nt} \tag{14}$$

$$\tau_{ty} = K_3\tau_{3ty} \tag{15}$$

where we have denoted σ_{1n}, σ_{2n}, etc., by

$$\sigma_{1n} = \left(3\cos\frac{\theta}{2} + \cos\frac{5\theta}{2}\right)\Big/ 4\sqrt{2\pi r} \tag{16}$$

$$\sigma_{2n} = -\left(7\sin\frac{\theta}{2} + \sin\frac{5\theta}{2}\right)\Big/ 4\sqrt{2\pi r} \tag{17}$$

$$\sigma_{1t} = \frac{2\nu}{\sqrt{2\pi r}}\cos\frac{\theta}{2} \tag{18}$$

$$\sigma_{2t} = -\frac{2\nu}{\sqrt{2\pi r}}\sin\frac{\theta}{2} \tag{19}$$

$$\sigma_{1y} = \frac{1}{4\sqrt{2\pi r}}\left(5\cos\frac{\theta}{2} - \cos\frac{5\theta}{2}\right) \tag{20}$$

$$\sigma_{2y} = -\frac{1}{4\sqrt{2\pi r}}\left(\sin\frac{\theta}{2} - \sin\frac{5\theta}{2}\right) \tag{21}$$

$$\tau_{3ty} = \frac{\cos\theta/2}{\sqrt{2\pi r}} \tag{22}$$

$$\tau_{3nt} = -\frac{\sin\theta/2}{\sqrt{2\pi r}} \tag{23}$$

$$\tau_{1ny} = \frac{-1}{4\sqrt{2\pi r}}\left(\sin\frac{\theta}{2} - \sin\frac{5\theta}{2}\right) \tag{24}$$

$$\tau_{2ny} = \frac{1}{4\sqrt{2\pi r}}\left(3\cos\frac{\theta}{2} + \cos\frac{5\theta}{2}\right) \tag{25}$$

Here σ_{1t} is the coefficient of K_1 in the expression for σ_t, etc. In a similar fashion the displacements can also be expressed as

$$u_n = K_1u_{1n} + K_2u_{2n} \tag{26}$$

$$u_t = K_3u_{3t} \tag{27}$$

$$u_y = K_1u_{1y} + K_2u_{2y} \tag{28}$$

where

$$u_{1n} = \frac{1}{2G}\sqrt{\frac{2r}{\pi}}\cos\frac{\theta}{2}\left(\sin^2\frac{\theta}{2} + 1 - 2\nu\right) \tag{29}$$

$$u_{2n} = \frac{1}{2G}\sqrt{\frac{2r}{\pi}}\sin\frac{\theta}{2}\left(2 - 2\nu + \cos^2\frac{\theta}{2}\right) \tag{30}$$

$$u_{1y} = \frac{1}{2G}\sqrt{\frac{2r}{\pi}}\sin\frac{\theta}{2}\left(2 - 2\nu - \cos^2\frac{\theta}{2}\right) \tag{31}$$

$$u_{2y} = -\frac{1}{2G}\sqrt{\frac{2r}{\pi}}\cos\frac{\theta}{2}\left(1 - 2\nu - \sin^2\frac{\theta}{2}\right) \tag{32}$$

$$u_{3t} = \frac{1}{G}\sqrt{\frac{2r}{\pi}}\sin\frac{\theta}{2} \tag{33}$$

Here G is the shear modulus and ν is Poisson's ratio. It is interesting to note that the σ_n, σ_t, and σ_y stresses satisfy the relationship

$$\sigma_t = \nu(\sigma_n + \sigma_y) \tag{34}$$

which shows that a state of plane strain exists near the crack front.

In order to evaluate the "primitive" stiffness matrix for this element we first need to consider the strain energy V of the element which, in the present case, is given by

$$V = \frac{1}{2E}\int\int\int\{(1-\nu^2)(\sigma_n + \sigma_y)^2 + 2(1+\nu)(\tau_{ny}^2 - \sigma_n\sigma_y)\}J(r,\theta,\phi)\,dr\,d\theta\,d\phi + \\ + \frac{1}{2G}\int\int\int(\tau_{nt}^2 + \tau_{ty}^2)J(r,\theta,\phi)\,dr\,d\theta\,d\phi \tag{35}$$

where E is Young's modulus and

$$J(r,\theta,\phi) = r(\pi_0^4 + r\cos\theta\, ab(\pi_0)) \tag{36}$$

We now need to assume a functional form for the dependence of the stress intensity factors upon ϕ within the element. Perhaps the simplest, but by no means the only, such approach is to assume that K_1, K_2, and K_3 vary linearly within the element, i.e.

$$K_1(\phi) = K_{1e}\psi_1(\phi) + K_{1e+1}\psi_2(\phi) \tag{37}$$

with similar expressions for $K_2(\phi)$ and $K_3(\phi)$. Here

$$\psi_1(\phi) = 1 - \frac{(\phi - \phi_e)}{\phi_{e+1} - \phi_e} \tag{38}$$

$$\psi_2(\phi) = \frac{\phi - \phi_e}{\phi_{e+1} - \phi_e} \tag{39}$$

This returns the values of K_{1e}, K_{2e} and K_{3e} at the plane $\phi = \phi_e$ and the values of K_{1e+1}, K_{2e+1}, and K_{3e+1} at the plane $\phi = \phi_{e+1}$. Thus in addition to the degrees of freedom u_0, v_0, w_0, ω_{xz}, ω_{yz}, ω_{xy} associated with rigid body motion the special element will have as degrees of freedom the values of K_{1e}, K_{2e}, K_{3e}, K_{1e+1}, K_{2e+2}, K_{3e+1}. The vector $\boldsymbol{\lambda}$ which contains these degrees of freedom we define as

$$\boldsymbol{\lambda}^T = [K_{1e}, K_{1e+1}, K_{2e}, K_{2e+1}, K_{3e}, K_{3e+1}, u_0, v_0, w_0, \omega_{xy}, \omega_{xz}, \omega_{yz}] \tag{40}$$

As in References 3 and 4 the "primitive" stiffness matrix K^e for this element may now be obtained by differentiating the strain energy with respect to each of its elemental degrees of freedom, i.e.

$$K^e\boldsymbol{\lambda} = \frac{\partial v}{\partial \boldsymbol{\lambda}} \tag{41}$$

On carrying out this differentiation it is found that each element of the stiffness matrix is of the form

$$K_{ij} = \frac{1}{E}\int\int\int F_{ij}J\,dr\,d\theta\,d\phi \tag{42}$$

where for $i, j \leq 2$

$$F_{ij} = \psi_i\psi_j\{(1-\nu^2)(\sigma_{1n}+\sigma_{1y})^2 + 2(1+\nu)\times(\tau_{1ny}{}^2 - \sigma_{1n}\sigma_{1y})\}$$

for $i \leqslant 2$, $3 \leqslant j \leqslant 4$

$$F_{ij} = \tfrac{1}{2}\psi_i\psi_{j-2}\{2(1-\nu^2)(\sigma_{1n}+\sigma_{1y})(\sigma_{2n}+\sigma_{2y}) + 2(1+\nu)(2\tau_{1ny}\tau_{2y} - \sigma_{1n}\sigma_{2y} - \sigma_{2n}\sigma_{1y})\}$$

for $3 \leqslant i, j \leqslant 4$

$$F_{ij} = \psi_{i-2}\psi_{j-2}\{(1-\nu^2)(\sigma_{2n}+\sigma_{2y})^2 + 2(1+\nu)(\tau_{2ny}{}^2 - \sigma_{2n}\sigma_{2y})\}$$

for $5 \leqslant i, j \leqslant 6$

$$F_{ij} = \psi_{i-4}\psi_{-4}2(1+\nu)\{\tau_{3nt}{}^2 + \tau_{3ty}{}^2\} \tag{43}$$

and

$$F_{ji} = F_{ij} \tag{44}$$

for all values of i, j given above while for all other values of i, j

$$F_{ij} = 0 \tag{45}$$

Here the triple integral is over the value of the special element and is, in general, evaluated numerically.

So far we have primarily been concerned with determining the stiffness matrix for the element treating the vector $\boldsymbol{\lambda}$ as the vector containing the degrees of freedom of the element. However, in order to develop an element which is readily compatible with most finite element packages it is necessary to derive the stiffness matrix treating the nodal displacements, at each of the nodes of the element, as the basic degrees of freedom. This can be done using the procedure developed in References 3 and 4.

Let us define the displacements in the x, y, and z directions by u, v, and w respectively. Then u, r, and w are related to u_n, u_t, and u_y as follows

$$u = u_n\cos\theta' + u_t\sin\theta' + u_0 + z\omega_{xz} - y\omega_{xy} \tag{46}$$

$$v = u_y + v_0 - z\omega_{zy} + x\omega_{xy} \tag{47}$$

$$w = u_n\sin\theta' - u_t\cos\theta' + w_0 + y\omega_{zy} - x\omega_{xz} \tag{48}$$

If the special element is chosen to have m modes then, at the ith node ($1 \leqslant i \leqslant m$) the cartesian displacements u_i, v_i, and w_i are related to u_n, u_y, and u_t by the formulae

$$u_i = u_n(r_i, \theta_i, \phi_i)\cos\theta_i' + u_t(r_i, \theta_i, \phi_i)\times\sin\theta_i' + u_0 + z_i\omega_{xz} - y_i\omega_{xy} \tag{49}$$

$$v_i = u_y(r_i, \theta_i, \phi_i) + v_0 - z_i\omega_{zy} + x_i\omega_{xy} \tag{50}$$

$$w_i = u_n(r_i, \theta_i, \phi_i)\sin\theta_i' - u_t(r_i, \theta_i, \phi_i)\times\cos\theta_i' + w_0 + y_i\omega_{zy} - x_i\omega_{xz} \tag{51}$$

where r_i, θ_i, ϕ_i are the curvilinear co-ordinates of the ith node on the boundary of the special element and x_i, y_i, and z_i are the cartesian co-ordinates of this node. Substitution of the expressions for u_n, u_t, and u_y, as given by Equations (26), (27), and (28), into Equations (49), (50), and (51) now results in a matrix equation of the form

$$L\boldsymbol{\lambda} = \boldsymbol{\delta} \tag{52}$$

where

$$\boldsymbol{\delta}^T = [u_1, v_1, w_1, u_2, v_2, w_2 \ldots v_m, w_m] \tag{53}$$

and L is a transformation matrix of dimensions $3m \times 12$. Since, for the sake of accuracy, the special element will be coupled to the rest of the structure at more points than there are degrees of freedom we use the least squares technique to minimize the discontinuity of the displacements across the boundary of the special element. This procedure is described in detail in References 3 and 4 and gives

$$\boldsymbol{\lambda} = (L^TL)^{-1}L^T\boldsymbol{\delta} \tag{54}$$

so that when the nodal displacements u_i, v_i, and w_i are considered as the degrees of freedom then the element stiffness matrix becomes $(L^TL)^{-1T}K(L^TL)^{-1}L^T$.

This formulation of the stiffness matrix may be used in conjunction with any of the standard finite element routines.

When recovering the values of the stress intensity factors we may either use the least squares solution, given in Equation (54), or alternatively we may adopt the procedure suggested by Blackburn and Helen[5] which uses nodes on the crack face. Of the two, the approach suggested in Reference 5 is perhaps the most straightforward.

3. ILLUSTRATIVE EXAMPLES

As illustrative examples of this approach let us consider the following problems. An enclosed penny shaped crack, of radius 25·4 mm, located with its origin at the centre of a square bar of aluminium, the length of the sides of the bar being 254 mm, and a semi-circular surface flaw of radius 25·4 mm centrally located in a rectangular bar of aluminium with dimensions 254 mm × 254 mm × 127 mm (see Fig. 3). In each case the bar is subject to a uniform tensile stress of 68·9 MPa.

In analysing the internal penny shaped flaw the symmetry conditions enabled us to model only one quarter of the bar. The mesh consisted of 203 nodal points with 141 elements and 3 special elements each of which is rectangular in plan view and has 10 nodal points. This mesh is shown in Figure 4.

The value of the stress intensity factor K_1 at points A and B, as shown in Figure 3*a*, was found to be $K_1/\sigma\sqrt{a} = 1{\cdot}20$ as against the theoretical value of $K_1/\sigma\sqrt{a} = 1{\cdot}13$, given in Reference 6, for a crack in an infinite elastic body and the value of $K_1/\sigma\sqrt{a} = 1{\cdot}15$ allowing for a magnification of the previous value due to finite width effects but not allowing for the additional magnification due to back surface effects. Here σ is the applied stress (= 68·9 MPa) and a is the radius of the crack (= 25·4 mm).

When analysing the semi-circular surface flaw problem use may also be made of the symmetry considerations so that the mesh used in the previous problem may also be utilized for the present problem.

The value of the stress intensity factor obtained at point B, the point of deepest penetration, was $K_1/\sigma\sqrt{a} = 1{\cdot}22$ as against the value of 1·18 given by Smith[7] for a semi-circular surface flaw in a semi-infinite block and the value of 1·20 allowing for a magnification of this value due to back face effects. The value of the stress intensity factor obtained at point A, on the free surface, was $K_1/\sigma\sqrt{a} = 1{\cdot}48$ as against the value of 1·39 for a semi-infinite block and the value of 1·41 allowing for a magnification due to finite width effects.

In both cases the accuracy of the solution is sufficient for most engineering purposes and the error was never greater than 4·6%. Furthermore in the case of a through crack the analysis is similar to that given by Hilton,[8] and coincides with the analysis presented by the authors in References 3 and 4 in the case of a through crack in a thin sheet.

One very important fact, which should be mentioned, is that for a part circular crack the volume integration in Equation (42) simplifies to the extent that the r and θ integration may be carried out analytically. This leaves only the integration with respect to ϕ to be evaluated numerically. This simplification is primarily due to the fact that for a part circular crack $a = b$, and

$$J = r(a + r\cos\theta) \tag{55}$$

$$\theta' = \phi \tag{56}$$

$$\pi_0 = a^2 \tag{57}$$

Full details of this simplified approach are given in the Appendix for the case of mode 1 fracture only.

Here we have specifically concentrated on elliptical flaws since this shape is perhaps the most common encountered in practice. Indeed the geometry of most flaws may be thought of as being either part of a penny shaped flaw or consisting of sections each of which may be approximated as part of a penny shaped flaw.

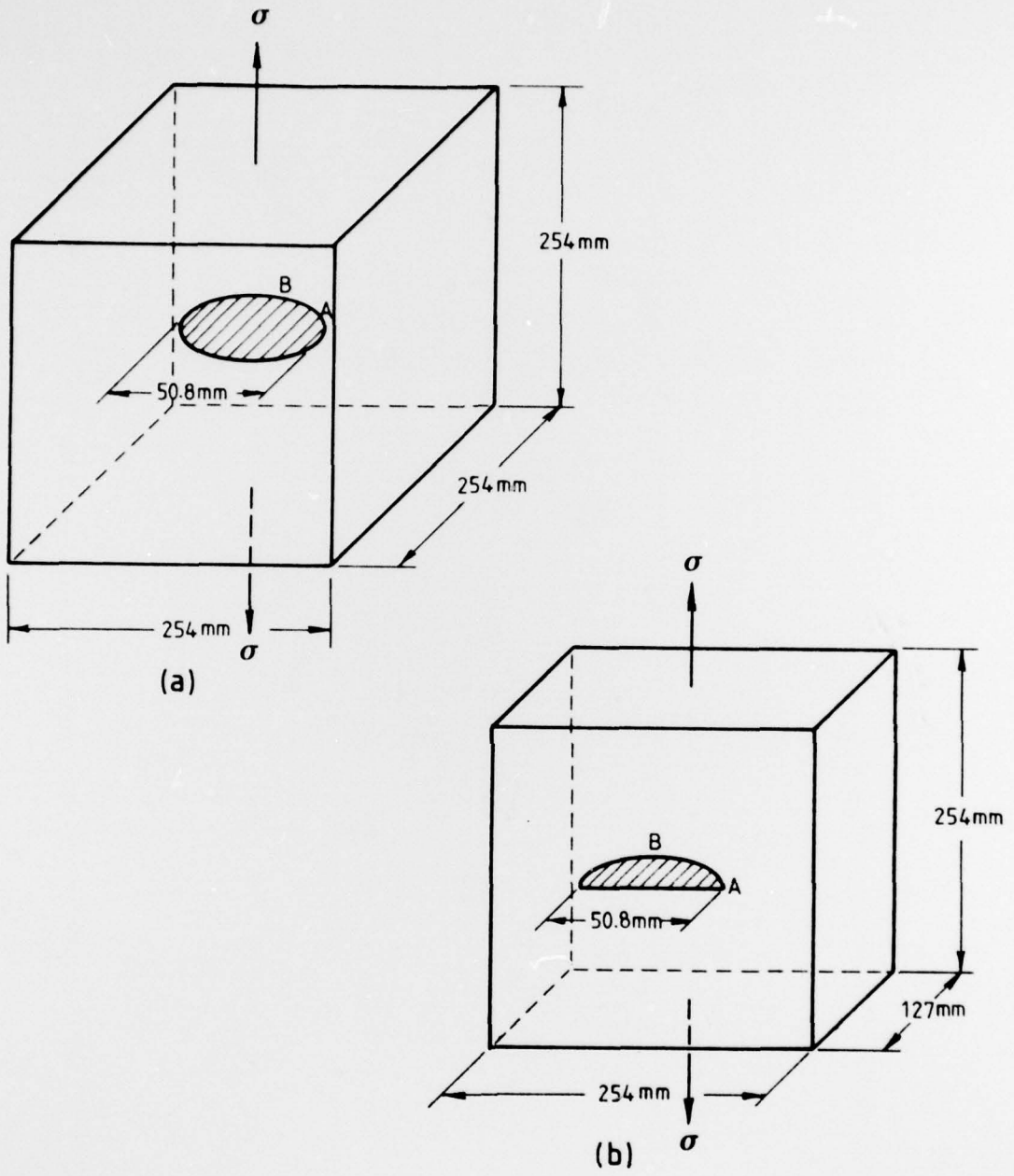

FIG. 3. GEOMETRY OF THE SURFACE CRACK AND THE EMBEDDED PENNY SHAPED FLAW.

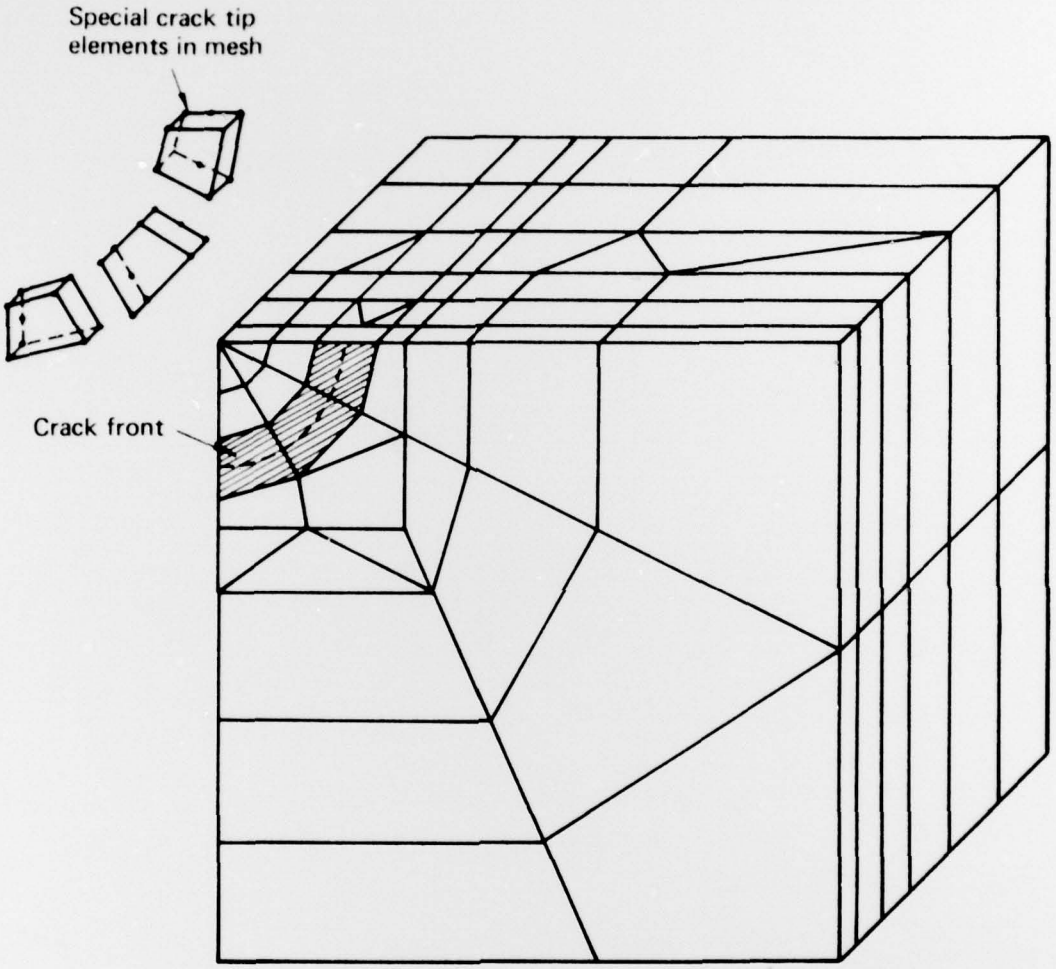

FIG. 4. FINITE ELEMENT REPRESENTATION.

4. FREE SURFACE STRESS CONDITIONS

When evaluating the stress intensity factors associated with a surface flaw it is of considerable importance to assess correctly the effect that the surface has on the stress intensity factors at the crack free surface intersection, see Jones.[9]

Indeed in recent years a considerable effort has been spent on evaluating the stress distribution at the intersection of a crack with a free surface. The work of Hartranft and Sih[10] is particularly significant as they showed that, in three-dimensional elasticity, the near crack stress field is in a state of plane strain, i.e.

$$\sigma_z = \nu(\sigma_x + \sigma_y) \tag{58}$$

where x, y, and z are a system of cartesian co-ordinates, as introduced in Section 1, the z axis being in the thickness direction. Hence for surface flaws the stress conditions

$$\sigma_z = \tau_{xz} = \tau_{yz} = 0 \tag{59}$$

on the free surface were thought by Sih[11] to force the stress intensity factor K_1, in the case of mode 1 fracture, to vanish at the free surface. Indeed this approach has led, in recent numerical studies by Hilton,[8] to enforce $K = 0$, at a free surface, as a boundary condition. This is in contrast to the work of Blackburn and Helen[5] where no resriction was placed on the value of K_1 at the free surface.

Whilst setting $K_1 = 0$ at the surface may not dramatically change the maximum value of K_1, obtained in those problems in which the crack is a through crack and for which the maximum value of K_1 occurs at the centre of the crack front, it is nevertheless a very important point. For surface flaws the value of K_1 at a free surface may have a significant effect on the maximum value achieved by K_1, and in some instances $K_{1_{max}}$ may even occur at the free surface.

Let us now examine the implication of setting $K_1 = 0$ at a free surface. Using Sih's[12] criterion for crack growth the onset of crack growth is determined by the value of the strain energy density function S, where S is defined as

$$S = \lim_{r \to 0} \frac{r}{2} (\sigma_x \epsilon_x + \sigma_y \epsilon_y + \sigma_z \epsilon_z + \tau_{xy}\gamma_{xy} + \tau_{xz}\gamma_{xz} + \tau_{yz}\gamma_{yz}) \tag{60}$$

and where, as before, $r = 0$ is the crack front.

At the intersection of a crack with a free surface the value of S reduces to

$$S = \lim_{r \to 0} \frac{r}{2} (\sigma_x \epsilon_x + \sigma_y \epsilon_y + \tau_{xy}\gamma_{xy}) \tag{61}$$

which for plane strain reduces to

$$S = a_{11}K_1^2 + 29_{12}K_1K_2 + a_{22}K_2^2 + a_{33}K_3^2 = a_{11}K_1^2 \text{ (for mode 1 fracture)} \tag{62}$$

where

$$a_{11} = \frac{1}{16\pi G}(3 - 4\nu - \cos\alpha)(1 + \cos\alpha) \tag{63}$$

$$a_{12} = \frac{2}{16\pi G}\sin\alpha(\cos\alpha - 1 + 2\nu) \tag{64}$$

$$a_{22} = \frac{1}{16\pi G}\{4(1 - \nu)(1 - \cos\alpha) \tag{65}$$

$$+ (1 + \cos\alpha)(3\cos\alpha - 1)\} \tag{66}$$

$$a_{33} = \frac{1}{4\pi G} \tag{67}$$

Here α defines the direction of crack growth. Consequently adopting the requirement that K_1 vanishes at a free surface forces S to vanish at the surface which subsequently prohibits the mathematical requirement for crack growth from being satisfied. Examining Equation (62) we see that in order for the value of S to be non-zero at the crack front–free surface inter-

section the σ_x, σ_y and τ_{xy} stresses must be non-zero and singular. This is possible only if a state of plane stress exists in the vicinity of the intersection. Indeed if a state of plane stress does exist at the crack front close to the free surface then the σ_z and τ_{yz}, τ_{xz} stresses are zero whilst a non-zero stress intensity factor may be associated with the σ_x, σ_y, and τ_{xy} stresses. Furthermore, since on the free surface

$$\sigma_z = \tau_{xz} = \tau_{yz} = 0 \tag{68}$$

Then, provided that the stresses are continuous functions of z, the plane stress approximation must be sufficiently accurate for a thin layer of material adjacent to the crack front–free surface intersection.

This now suggests an alternative numerical model to those previously developed for the study of through, or surface, cracks in which the crack tip element next to the free surface is developed assuming a state of plane stress within the cracked element. The other crack tip elements may be as derived in Section 2 above or as described in either of References 8 or 5.

Let us now examine the procedure, which was adopted in Reference 5, where the stress intensity factor was not forced to be zero at a free surface. This approach appears to be in agreement with the experimental results of Marrs and Smith.[13] They used the method of frozen slices, and found that, in the thin slice adjacent to the free surface, the value of stress intensity factor was non-zero. They subsequently concluded that if the stress intensity factor is zero at a free surface then the layer in which it shrinks to zero must be very thin; indeed it must be too thin to affect their experimental results. Hence when using a numerical method, in which the crack tip element is in a state of plane strain, this would imply that relatively little error will occur if this layer is neglected and the value of the stress intensity factor is allowed to be non-zero at the free surface. A further increase in the accuracy of the plane strain solution will occur if, having calculated the surface displacements using the plane strain assumption, the stress intensity factors, at the surface only, are derived from the surface displacements using the plane stress relationships. If, for example, this approach is applied to the semicircular flaw problem discussed in the previous section then the value of $K_1/\sigma\sqrt{a}$ at the surface, evaluated using the plane stress assumption reduces from 1·48 to 1·33 and differs only slightly from the value of 1·22 obtained at the point of maximum penetration.

5. CONCLUSION

In this study we have developed a simple finite element method for analysing flaws in a three-dimensional body, which in the case of a semicircular surface flaw, or an embedded penny shaped crack, under tension yields values for the stress intensity factor which are sufficiently accurate for most engineering purposes. The special element may be of any shape and for circular, or part circular flaws, requires little reliance upon numerical integration routines.

The special element may also be readily incorporated as a routine in any standard finite element program.

Although, within an element, the present analysis assumes a linear variation of the stress intensity factors along the crack front the analysis is sufficiently flexible so as to allow this assumption to be replaced by any other prescribed functional variation along the crack front.

REFERENCES

1. Sih, G. C., and Liebowitz, H. Mathematical Fundamentals—Fracture, vol. 2. Academic Press, N.Y., 1969.

2. Gallagher, R. H. A review of finite element techniques in fracture mechanics. Proceedings of the First Int. Conf. in Numerical Methods in Fracture Mechanics (A. R. Luxmore and D. R. J. Owen, eds), 1977.

3. Jones, R., and Callinan, R. J. A finite element method for calculating the stress intensity factors in cracked sheets. ARL Struc. Rept. 360, 1976. (Also presented at 14th IUTAM Congress at Delft, 1976.)

4. Jones, R., and Callinan, R. J. On the use of special crack tip elements in cracked elastic sheets. *Int. J. Fracture*, vol. 13, 1, pp. 51–64, 1977.

5. Blackburn, W. S., and Helen, T. K. Calculation of stress intensity factors in three dimensions by finite element methods. *Int. J. Numerical Methods in Energy*, vol. 11, 211–29, 1977.

6. Kassir, M. K., and Sih, G. C. Three-dimensional stress distribution around an elliptic crack under arbitrary loading. *J. Appl. Mech.*, pp. 601–609, 1966.

7. Smith, F. W. The elastic analysis of the part circular surface flaw problem by the alternating method. The Surface crack. ASME, 79–124, 1972.

8. Hilton, P. D. A specialized finite element approach for three-dimensional crack problems. Mechanics of Fracture, vol. III, pp. 273–97. (G. C. Sih, ed.) Noordhoff Int. Publishing, Leyden, 1973.

9. Jones, R. On the state of stress at a crack free surface intersection. *Int. J. Fracture*, October 1978 (in press).

10. Hartranft, R., and Sih, G. C. The use of eigenfunction expansions in three-dimensional crack problems. *Journal of Maths and Mech.*, 19, pp. 123–38, 1969.

11. Sih, G. C. A review of the three-dimensional stress problem for a cracked plate. *Int. J. Fracture Mechanics*, 7. pp. 39–61, 1971.

12. Sih, G. C. Methods of Analysis and Solutions of Crack Problems, pp. xxi–xlv. (G. C. Sih, ed.) Noordhoft Int. Publishing, Leyden, The Netherlands, 1973.

13. Marrs, G. R., and Smith, C. W. A study of local stresses near surface flaws in bending fields. ASTM STP513, pp. 22–36, 1971.

14. Ryshik, I. M., and Gradstein, I. S. Tables of series products and integrals. Deutscher Verlag das Wissenschaft, Berlin, 1957.

APPENDIX

For mode 1 fracture the only non-zero values of the stress intensity factors are K_{1e} and K_{1e+1} so that the only values of K_{ij} which are required are for $i, j \leqslant 2$. In this case substituting for σ_{1n}, σ_{1y}, and τ_{1ny} into Equation (42) gives

$$K_{ij} = \frac{1}{8G\pi}\int\int\int \psi_i\psi_j\{(3 - 4\nu - \cos\theta)(1 + \cos\theta)(a + r\cos\theta)\}\mathrm{d}r\mathrm{d}\theta\mathrm{d}\phi \qquad (a)$$

On the surface of the special element, shown in Figure 2, the radius vector r takes the value

$$r = rr(\phi, \phi_e, rr_e)/\cos\theta \qquad (b)$$

for $0 \leqslant \theta \leqslant \theta^{\circ}$, and

$$r = y_0/\sin\theta \qquad (c)$$

for $\theta^{\circ} \leqslant \theta \leqslant \theta'$, and

$$r = rl(\phi, \phi_e, rl_e)/\cos\theta \qquad (d)$$

for $\theta' \leqslant \theta \leqslant \pi$. Here y_0 is the thickness of the element in the y direction, rr_e and rl_e are the distances of the sides of the special element from the crack front on the plane $\phi = \phi_e$ and rr and rl are the distances of the sides of the special element from the crack front on the plane $\phi = \phi$, while θ° and θ' are the angles at which the sides of the special element intersect. The functional form of rr and rl is given below, viz.

$$rr = (a(\sin\phi_e - \sin\phi) + t(\cos\phi_e - \cos\phi)) + rr_e(\sin\phi_e + t\cos\phi_e)/(\sin\phi + t\cos\phi) \qquad (e)$$

and

$$rl = (a(\sin\phi_e - \sin\phi + t(\cos\phi_e - \cos\phi)) - rl_e(\sin\phi_e + t\cos\phi_e))/(\sin\phi + t\cos\phi) \qquad (f)$$

where

$$t = \frac{\sin\phi_e - \sin\phi_{e+1}}{\cos\phi_{e+1} - \cos\phi_e} \qquad (g)$$

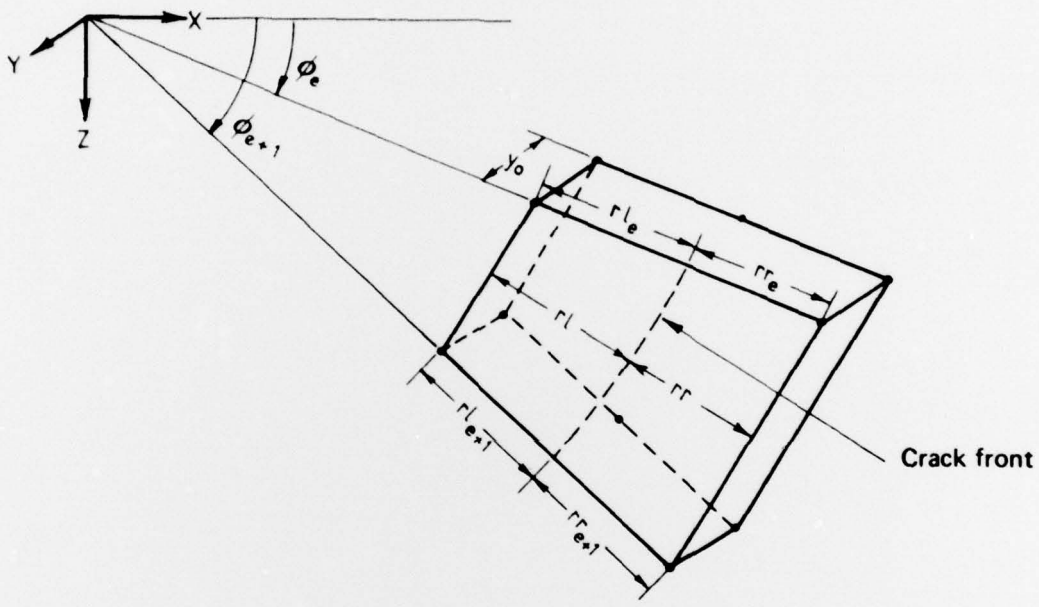

FIG. 5. ELEMENT GEOMETRY.

Consequently after integrating Equation (*a*) with respect to r we obtain

$$K_{ij} = \frac{1}{8\pi G}\int_{\phi_{e-1}}^{\phi_{e+1}} \phi_i \psi_j \int_0^{\pi} I(\theta)\mathrm{d}\theta\mathrm{d}\phi \qquad (h)$$

where for $0 \leqslant \theta \leqslant \theta^{\circ}$

$$I(\theta) = \frac{rr}{\cos\theta}\left(3 - 4\nu - \cos\theta\right)\left(1 + \cos\theta\right)\left(a + \frac{rr}{2}\right) = I_1(\theta) \qquad (i)$$

for $\theta^{\circ} \leqslant \theta \leqslant \theta'$

$$I(\theta) = \frac{y_0}{\sin\theta}\left(3 - 4\nu - \cos\theta\right)\left(1 + \cos\theta\right)\left(a + \frac{y_0\cot\theta}{2}\right) = I_2(\theta) \qquad (j)$$

for $\theta' \leqslant \theta \leqslant \pi$

$$I(\theta) = \frac{rl}{\cos\theta}\left(3 - 4\nu - \cos\theta\right)\left(1 + \cos\theta\right)\left(a + \frac{rl}{2}\right) = I_3(\theta) \qquad (k)$$

Here the integral with respect to θ may be considered as three separate integrals, i.e.

$$\int_0^{\pi} I(\theta)\mathrm{d}\theta = \int_0^{\theta^{\circ}} I_1\mathrm{d}\theta + \int_{\theta^{\circ}}^{\theta'} I_2\mathrm{d}\theta + \int_{\theta}^{\pi} I_3\mathrm{d}\theta \qquad (l)$$

Substituting into Equation (*l*) the expressions for I_1, I_2, and I_3 as given by Equations (*i*), (*j*), and (*k*) we find that

$$\int_0^{\theta^{\circ}} I_1\mathrm{d}\theta = \left(a + \frac{rr}{2}\right)rr\left[\left(3 - 4\nu\right)\int_0^{\theta}\frac{\mathrm{d}\theta}{\cos\theta} - \sin\theta_0 + 2\left(1 - 2\nu\right)\theta^{\circ}\right] \qquad (m)$$

$$\int_{\theta^{\circ}}^{\theta'} I_2\mathrm{d}\theta = ay_0\left[\left(3 - 4\nu\right)\int_{\theta^{\circ}}^{\theta'}\frac{\mathrm{d}\theta}{\sin\theta} + 2\left(1 - 2\nu\right) \times \ln\left(\frac{\sin\theta'}{\sin\theta^{\circ}}\right) - \int_{\theta^{\circ}}^{\theta'}\frac{\cos^2\theta}{\sin\theta}\mathrm{d}\theta\right]$$

$$+ \frac{y_0^2}{2}\left[\left(3 - 4\nu\right)\left(\frac{1}{\sin\theta^{\circ}} - \frac{1}{\sin\theta'}\right) + 2\left(1 - 2\nu\right)\int_{\theta^{\circ}}^{\theta'}\frac{\cos^2\theta}{\sin^2\theta}\mathrm{d}\theta - \int_{\theta}^{\theta'}\frac{\cos^3\theta}{\sin^2\theta}\mathrm{d}\theta\right] \qquad (n)$$

$$\int_{\theta'}^{\pi} I_3\mathrm{d}\theta = rl\left(a + \frac{rl}{2}\right)\left[\left(3 - 4\nu\right)\int_{\theta'}^{\pi}\frac{\mathrm{d}\theta}{\cos\theta} + \sin\theta_1 + 2\left(1 - 2\nu\right)\left(\pi - \theta'\right)\right] \qquad (o)$$

Equations (*m*), (*n*), and (*o*) contain several terms in integral form. These can be readily evaluated using the formulae

$$\int\frac{\mathrm{d}\theta}{\cos\theta} = \ln\tan\left(\frac{\pi}{4} + \frac{\theta}{2}\right) \qquad (p)$$

$$\int\frac{\mathrm{d}\theta}{\sin\theta} = \ln\tan\left(\theta/2\right) \qquad (q)$$

$$\int\frac{\sin^2\theta}{\cos^2\theta}\mathrm{d}\theta = \tan\theta - \theta \qquad (r)$$

$$\int\frac{\cos^2\theta}{\sin^2\theta}\mathrm{d}\theta = -(\cot\theta + \theta) \qquad (s)$$

$$\int\frac{\cos\theta}{\sin^2\theta}\mathrm{d}\theta = -\frac{1}{\sin\theta} \qquad (t)$$

$$\int\frac{\cos\theta}{\sin^2\theta}\mathrm{d}\theta = -\left(\sin\theta + \frac{1}{\sin\theta}\right) \qquad (u)$$

$$\int \frac{\cos^2\theta}{\sin\theta}\,d\theta = \ln\left(\tan\left(\frac{\theta}{2}\right)\right) + \cos\theta \qquad (v)$$

These formulae, and several other useful formulae, may be found on pages 96 and 97 of Reference 14.

Having thus evaluated the integrals I_1, I_2, and I_3 then, in order to compute the values of K_{ij}, it is only necessary to perform the integration with respect to ϕ. Because of the complexity of the integrand it is not possible to perform this integration analytically so that the integration with respect to ϕ is performed numerically.

As a result of this analysis we see that when the crack front forms part of a circle, then in order to calculate the stiffness matrix, only the integration with respect to ϕ needs to be carried out numerically.

DOCUMENT CONTROL DATA SHEET

Security classification of this page: Unclassified

1. Document Numbers
   (a) AR Number:
   AR-001-319
   (b) Document Series and Number
   Structures Report 374
   (c) Report Number:
   ARL-Struc-Report-374

2. Security Classification
   (a) Complete document:
   Unclassified
   (b) Title in isolation:
   Unclassified
   (c) Summary in isolation:
   Unclassified

3. Title: A SPECIAL CRACK TIP ELEMENT FOR THREE-DIMENSIONAL CRACK PROBLEMS

4. Personal Author(s):
   Rhys Jones
   Richard J. Callinan

5. Document Date:
   November, 1978

6. Type of Report and Period Covered:

7. Corporate Author(s):
   Aeronautical Research Laboratories

8. Reference Numbers
   (a) Task:
   AIR 78/164
   (b) Sponsoring Agency:
   Department of Defence (Air Office)

9. Cost Code: 21 1000

10. Imprint:
    Aeronautical Research Laboratories,
    Melbourne

11. Computer Program(s)
    (Title(s) and language(s)):

12. Release Limitations (of the document): Approved for public release

12-0. Overseas:	N.O.		P.R.	1	A		B		C		D		E	

13. Announcement Limitations (of the information on this page): No limitation

14. Descriptors:
    Cracking (fracturing)
    Cracks
    Fracture properties
    Stress analysis
    Stress concentration
    Stresses
    Finite element method

15. Cosati Codes: 2012

16.

ABSTRACT

This paper develops a finite element method for determining the stress intensity factors along the edge of a crack in an arbitrary three-dimensional body. A special element is placed around the crack front and in each special element the stresses and displacements are derived using the asymptotic nature of the stress and displacement fields near a crack tip.

The method is based on the authors' previous technique for evaluating the stress intensity factors in cracked sheets, and coincides with this method in the case of a through crack in a thin sheet. As illustrative examples the problems of a semicircular surface flaw and an internal penny shaped crack are considered. In each case the computed values of the stress intensity factors are in excellent agreement with known analytical results.

DISTRIBUTION

	Copy No.
AUSTRALIA	
Department of Defence	
Central Office	
Chief Defence Scientist	1
Deputy Chief Defence Scientist	2
Superintendent, Science and Technology Programs	3
Australian Defence Scientific and Technical Representative (UK)	4
Counsellor, Defence Science	5
Defence Library	6
JIO	7
Assistant Secretary, DISB	8–23
Aeronautical Research Laboratories	
Chief Superintendent	24
Superintendent, Structures Division	25
Divisional File, Structures Division	26
Authors: R. Jones	27
R. J. Callinan	28
Library	29
B. C. Hoskin	30
Materials Research Laboratories	
Library	31
Defence Research Centre, Salisbury	
Library	32
Central Studies Establishment Information Centre	
Library	33
Engineering Development Establishment	
Library	34
RAN Research Laboratory	
Library	35
Navy Office	
Naval Scientific Adviser	36
Army Office	
Army Scientific Adviser	37
Royal Military College	38
US Army Standardisation Group	39
Air Force Office	
Air Force Scientific Adviser	40
Aircraft Research and Development Unit	41
Engineering (CAFTS) Library	42
D. Air Eng.	43
HQ Support Command (SENGSO)	44

Department of Productivity

Government Aircraft Factories

Library		45

Department of National Resources

Secretary, Canberra		46

Department of Transport

Secretary/Library		47
Airworthiness Group (Mr. K. O'Brien)		48

Statutory, State Authorities and Industry

Australian Atomic Energy Commission (Director), NSW		49
CSIRO Mechanical Engineering Division (Chief)		50
CSIRO National Measurement Laboratory (Chief)		51
CSIRO Materials Science Division (Director)		52
Qantas, Library		53
Trans Australia Airlines, Library		54
Gas and Fuel Corporation of Victoria (Research Director)		55
Ministry of Fuel and Power (Secretary), Victoria		56
SEC Herman Research Laboratory (Librarian), Victoria		57
SEC of Queensland, Library		58
Ansett Airlines of Australia, Library		59
BHP Central Research Laboratories, NSW		60
BHP Melbourne Research Laboratories		61
Commonwealth Aircraft Corporation (Manager)		62
Commonwealth Aircraft Corporation (Manager of Engineering)		63
Hawker de Havilland Pty. Ltd. (Librarian), Bankstown		64
Hawker de Havilland Pty. Ltd. (Manager), Lidcombe		65

Universities and Colleges

Adelaide	Barr Smith Library	66
	Professor of Mechanical Engineering	67
Australian National	Library	68
Flinders	Library	69
James Cook	Library	70
La Trobe	Library	71
Melbourne	Engineering Library	72
Monash	Library	73
Newcastle	Library	74
New England	Library	75
New South Wales	Physical Sciences Library	76
	Professor R. A. A. Bryant, Mech. & Ind. Eng.	77
	Assoc. Prof. R. W. Traill-Nash, Struc. Eng.	78
Queensland	Library	79
Sydney	Prof. G. A. Bird, Aero. Eng.	80
	Prof. J. W. Roderick, Mech. Eng.	81
	Prof. R. Wilson, Applied Mathematics	82
Tasmania	Engineering Library	83
Western Australia	Library	84
	Prof. Allen-Williams, Mech. Eng.	85
	Dr. P. B. Chapman, Mathematics	86

SWEDEN

UNITED KINGDOM

Universities and Colleges

FLAW.

UNITED STATES OF AMERICA

NASA Scientific and Technical Information Facility		189
Sandia Group (Research Director)		190
American Institute of Aeronautics and Astronautics		191
Applied Mechanics Reviews		192
The John Crerar Library		193
The Chemical Abstracts Service		194
Boeing Co., Head Office		195
Boeing Co., Industrial Production Division		196
Cessna Aircraft Co. (Dr. D. W. Mallonee, Exec. Director)		197
Esso Research Laboratories (Director)		198
Lockheed Aircraft Co. (Director)		199
McDonnell Douglas Corporation (Director)		200
United Technologies Corp., Pratt & Whitney Aircraft Group		201
Battelle Memorial Institute, Library		202
Calspan Corporation		203

Universities and Colleges

Arizona	Library	204
Florida	Mark H. Clarkson, Dept. of Aero. Eng.	205
Illinois	Prof. N. M. Newmark, Talbot Labs.	206
Johns Hopkins	Prof. S. Corrsin, Dept. of Mech. Eng.	207
Massachusetts	Prof. W. A. Nash, Dept. of Civil Eng.	208
Princeton	Prof. G. L. Mellor	209
Stanford	Library, Department of Aeronautics	210
George Washington	Library	211
Wisconsin	Memorial Library, Serials Dept.	212
Brooklyn Institute of Polytechnology	Library, Polytech Aero. Labs.	213
California Institute of Technology	Library, Guggenheim Aero. Labs.	214

Spares 215–224


DATE
ILME
-8